Design and assessment of a new dual solid oxide fuel cell–gas turbine hybrid system

ZAHRA HAJIMOHAMMADI TABRIZ[1], **LEYLA KHANI**[1], **AND MOUSA MOHAMMADPOURFARD**[1,*]

[1] *Faculty of Chemical and Petroleum Engineering, University of Tabriz, Tabriz, Iran*
[*] *Corresponding author email: mohammadpour@tabrizu.ac.ir*

Manuscript received 14 February, 2022; revised 08 April, 2022; accepted 19 April, 2022. Paper no. JEMT-2202-1372.

Given the increasing energy demand, utilizing of high efficiency systems with low environmental impact seems necessary. Using new energy conversion methods such as electrochemical reactions is one of the solutions for this purpose. Fuel cells are devices for conducting continuous electrochemical reactions. The main goal of this research is to present and evaluate a new dual solid oxide fuel cell-gas turbine (SOFC-GT) plant. The proposed plant is designed for power generation. Energy, exergy, and environmental models are developed to simulate and investigate this system using EES software. The effect of key operating parameters on the system operation is studied. A similar single solid oxide fuel cell-gas turbine plant is also designed and evaluated for comparison with dual cell plant. The results of exergy analyses indicate that the largest exergy destruction for both single and dual cell cycles occurs in afterburner. In addition, the net rate of exergy destruction and energy efficiency attained by dual cell cycle are 384.1 kW and 63.93%, respectively. A comparison of dual cell with single cell cycle shows that the net power generation rate in the dual cell cycle is higher than the single cell cycle. In contrast, the net rate of exergy destruction in the dual cell system is more than single cell system. Dual SOFC-GT system is more environmentally friendly than a single SOFC-GT system because it has a lower carbon dioxide emission rate.

keywords: *Thermodynamic analysis, dual SOFC-GT cycle, exergy destruction rate, solid oxide fuel, carbon dioxide emission.*

http://dx.doi.org/10.22109/jemt.2022.329698.1372

1. INTRODUCTION

Energy is the first requirement in a variety of domestic and industrial applications. Fossil fuels, which are major sources of energy supply, are declining and have economic and environmental problems. For this reason, the importance of energy supply is felt more [1]. One of the proposed solutions to the energy problem is using new energy conversion methods such as electrochemical reactions. In this type of reaction, the chemical energy of the fuel is converted directly into electricity. One of the latest equipment that has been built for this purpose is the fuel cell (FCL). Unlike fuel combustion, in which the fuel burns to generate heat and later electrical and mechanical power, the fuel cell function is direct conversion. Fuel cells are devices for conducting continuous electrochemical reactions. Their advantages include low environmental impact, high energy efficiency, few moving parts, fuel diversity, and controllable operation size management [2]. The design of gas turbine power plants in a hybrid plant with solid oxide fuel cell (SOFC) has been studied in many articles[3]. Today, a configuration is often considered in which the gas turbine (GT) is placed after the SOFC afterburner, which forms the SOFC-GT system[4]. A review of the literature shows that this idea was first discussed by Ide et al. [5] who performed a comparative study on the net performances of 3 types of FCL-based power plants. The result showed that most of the inefficiencies are due to the irreversibility of fuel combustion. One way to improve efficiency is to avoid immediate contact between fuel and air, which occurs in fuel cells [6]. Some studies on the SOFC-GT cycle have been conducted to survey and improve the efficiency of these systems in previous years. Chan et al. [7] introduced a SOFC ± GT power generation (PG) plant that can achieve efficiencies of better than 60%. In another study, Chan et al.[8] introduced an IRSOFC–GT plant with internal reforming, which was fed with natural gas. Results showed that achieving more than 60% efficiency for this power system is possible. Calise et al.[9] proposed a partial and full load exergy assessment for a combined SOFC-GT system. The electrical efficiency can reach 65.4% i[10] analyzed a two-staged SOFCs- PG cycle in which the cells were arranged in series of high and low temperature SOFCs. The results revealed that the PG performance of the two-staged SOFCs system is 50.3%.
Most past studies in this field have numerically modeled SOFC performance.

However, a comprehensive review of the articles shows that the study of this hybrid system from the perspective of the SLT and the study of system irreversibility has received less attention [3]. Among the studies conducted in this field, we can mention these cases. Granovskii et al. [11]considered two different modes to compare the efficiency of the SOFC-GT cycle. The first approach was producing the steam required in a coupled gas turbine system. The latter was recycling part of the exhaust gases (EG) to the anode of the fuel cell stack. The results revealed that the second mode has higher energy and exergy efficiency (EEE), In contrast, the first plant can produce more power. Calise et al. [12] performed a thermodynamic analysis on a combined SOFC-GT plant. It was found that the effect of design variables, especially current density (CD) and the operating pressure on the plant is very high, so that in an optimal value of these variables, efficiency could be achieved close to 60% for a 1.5MW system. Studies on these systems have also moved towards being more environmentally friendly. The use of biofuels as input fuel to these cycles has been considered. Biofuels are renewable fuels that are less polluting and environmentally friendly because their use does not release hazardous substances into the environment [13]. For example, we can give two examples. Bang-Møller et al.[14] investigated a SOFC-GT combined plant with biomass fuel. They compare three cases in this article: a GT, a FCL, and a combined GT and FCL plant. Calculations reported the efficiency of these three systems as 28%, 36%, and 50%, respectively. Thus, the efficiency of a FCL is reported to be more than that of a gas turbine, and it is also apparent that the efficiency of the hybrid plant will be higher than that of both systems. In addition, they studied the effect of operational parameters on system efficiency. Wongchanapai et al.[15] analyzed a SOFC-GT combined cycle fed with biogas and investigated the effect of operating parameters, including the fuel utilization factor (FUF) and turbine inlet temperature, on the overall performance. Results showed that the influence of the FUF on SOFC and system efficiencies was not significant, but increasing turbine inlet temperature decreases the system electrical efficiency.

Recent studies in this area are also significant. Sghaier et al.[16] performed a parametric study on a SOFC-GT hybrid cycle. They studied the plant in terms of energy and exergy and applied the equations of electrochemical processes to their calculations. They also analyzed the effect of main parameters such as FUF and humidity on the efficiency of this SOFC-GT cycle. The results showed that integration of SOFC increases the overall efficiency of the plant significantly. Also, enhancing the ambient temperature and decreasing the humidity reduce the efficiency of the cycle. The FUF also has a negative impact on the cell voltage and temperature. Chitgar et al.[17] introduced a new SOFC-GT system for electricity, hydrogen, and water production. The exergy efficiency reported for this cycle was 54.2% at the optimum point. Beigzadeh et al.[18] conducted a thermodynamic analysis based on energy and exergy equations on a SOFC-GT system. They studied the impact of natural gas and biofuels, such as syngas, gasified biomass, and industrial and agricultural waste biogas as the fuel of the system. Further, they calculated the exergy destruction rate (EDR) of each equipment in the plant. Also, they studied the impact of applying several biofuels on the main parameters, such as EEE, amount of irreversibility for each equipment, compression ratio, operating pressure and temperature, and total production power have been analyzed. The results showed that natural gas fuel had the highest PG capacity of 879.03kW. Gasified biomass, had the lowest EDR of 101.2kW. Atsonios et al. [19] presented a new multigeneration system for power, cooling, and water production. They showed that SOFC-GT plants are the best option in terms of energy efficiency. Pan et al. [4] studied the supercritical recompression carbon dioxide system that has been adapted to the high temperature of the EG of the system to enhance PG. They have performed a 4E analysis on the system. Some of the key operating variables are studied, and an optimization is performed by a genetic algorithm. The results illustrated that the organic Rankine cycle, is most remarkable in terms of efficiency, because it can achieve the highest EEE. The values reported for EEE in a wide range of conditions were 72.74–73.55% and 70.22–71.01%, respectively. Khani et al.[20] Have designed a multigeneration system that supplies its required power from a gas turbine and a fuel cell. The thermodynamic and environmental efficiency of the system has been studied to determine the impact of key operational parameters on system performance. The results show that increasing the current density decreases the energy and exergy efficiency. System optimization using genetic algorithm reports exergy efficiency of 64%.

According to the above literature review, SOFC-GT cycles are taken into consideration in many papers. Hence, more developments are essential in this field. Although earlier studies have considered this hybrid system, the dual SOFC-GT cycle has not been presented yet. This work aims to assessment a new dual SOFC-GT plant for PG. The significance of this study is to provide a thermodynamic analysis for this cycle and compare it with a single SOFC-GT cycle from an energy and exergy perspective. In addition, to provide environmental insight into this assessment, carbon dioxide emission is calculated. Thus, the present study particularly focuses on the following objectives:

- Providing different parts of the software for the users in the form of modular layers, and showing the capability of each layer for a better EMS in a microgrid cluster.
- Design a hybrid dual SOFC-GT system for power generation.
- Perform energy, exergy, and environmental analyses on each component and the whole system for both dual SOFC-GT and single SOFC-GT using Engineering Equation Solver (EES) software.
- Investigate the impact of key operational parameters, including FUF and CD, on the system efficiency

2. PLANT DESCRIPTION

This section presents a description of the single and dual SOFC-GT plants

A. Single SOFC-GT plant

A schematic representation of the considered hybrid single SOFC-GT cycle is demonstrated in Fig. 1. This hybrid cycle includes a SOFC, a GT, two compressors for air (AC) and fuel (FC), an afterburner (AB), two heat exchangers (HX), and a mixer is considered. Pure methane as input fuel at state 5 enters the fuel compressor and air at state 1, enters the air compressor. They reach to fuel cell after passing through heat exchangers. To provide the steam needed for the reactions, part of the anode outlet will be mixed with incoming methane fuel. Cell-related electrochemical reactions take place inside the cell stack and generates electrical power. The fuel cell outlet streams are burned in the afterburner to eliminate the unreacted fuel and preheat the SOFC inlet air. The exit stream of the afterburner is

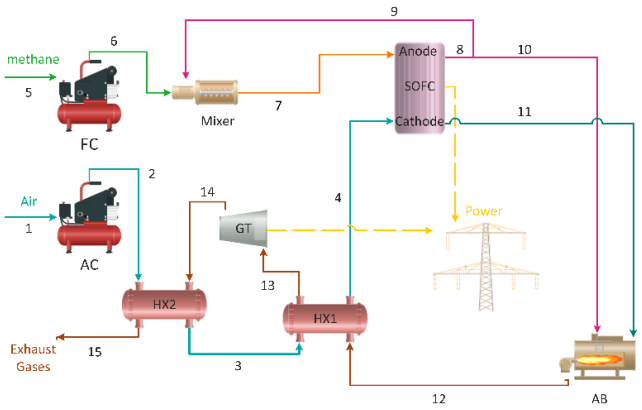

Fig. 1. Schematic representation of the Single SOFC-GT plant

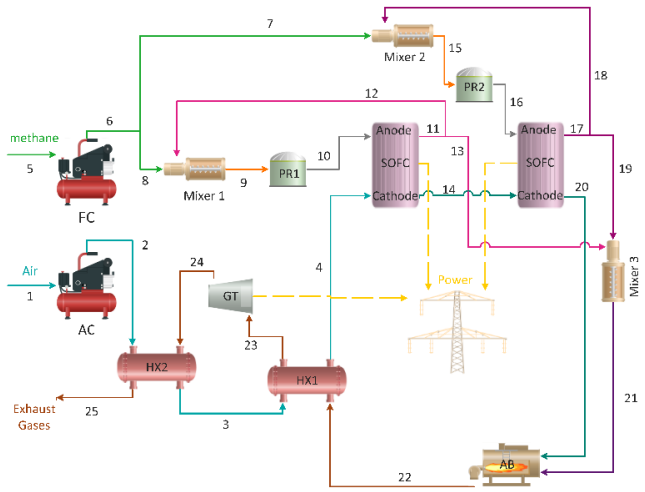

Fig. 2. Schematic representation of the dual SOFC-GT plant

sent to a GT to generate power and then leaves the system as EG.

B. Dual SOFC-GT system

A schematic diagram of the considered dual SOFC-GT cycle is demonstrated in Fig. 2. The hybrid system includes two SOFCs, a GT, two compressors for air and fuel, one afterburner, two heat exchangers, three mixers, and two pre reformers is considered. Pure methane as input fuel at state 5 enters the fuel compressor and air at state 1, enters the air compressor. They reach to fuel cell after passing through heat exchangers. To provide the steam needed for the reactions, part of the anode outlet will be mixed with incoming methane fuel. Cell-related electrochemical reactions take place inside the cell stack and generates electrical power. However, in this cycle, two pre-reformer units are considered to perform part of the reforming reaction. The same process is repeated for the second cell, except that the air entering this cell contains more nitrogen. The second SOFC cathode outlet with the first SOFC cathode outlet, and also the anode outlet streams are burned in the afterburner to eliminate the unreacted fuel and preheat the SOFC inlet air. The exit stream of the afterburner is sent to a GT to generate power and then leaves the system as EG.

3. MATHEMATICAL MODELING

This section discusses the thermodynamic analysis performed on each system component. Conservation of mass (COM), energy balance equation (EBE), and exergy relations, originating from the SLT, are applied. Furthermore, the SOFC stack equations are given for modeling its electrochemical reactions. The calculation was made by EES software as it contains the thermodynamic properties of system materials. The following assumptions are invoked for system modeling [21, 22]:

1. All the equipment operate in steady-state condition
2. The fuel of the FCL is methane gas.
3. The air considered here contains 79% N_2 and 21% O_2.
4. The gases are all assumed to be ideal gases (ig).
5. The temperature of cathode and anode outlets are equal to the FCL operating temperature.
6. The ambient temp. and press. are 25°C and 1.013 bar.
7. Heat loss to the environment is neglected.
8. No changes in the potential and kinetic energies and exergies.
9. Contact resistances in the FCL stack are negligible.
10. Pressure drops in the mixers and pipes are neglected.

A. General thermodynamic analysis

According to the COM, the mass balance equation is written as [23]:

$$\sum_i \dot{m_i} = \sum_e \dot{m_e} \quad (1)$$

The EBE based on the FLT for each component is expressed as follows [24]:

$$\dot{W}_{cv} - \dot{Q}_{cv} = \sum_i \dot{m}_i h_i - \sum_e \dot{m}_e h_e \quad (2)$$

Where $\dot{Q}$and$\dot{W}$ are heat transfer and work across system boundaries, and h is specific enthalpy of components. The EDR for each component, based on the exergetic analysis, is calculated as below [23]:

$$\dot{E}x_D = \sum (1 - \frac{T_0}{T_j})\dot{Q}_j - \dot{W}_{cv} + \sum \dot{E}x_i - \sum \dot{E}x_e \quad (3)$$

Where T_0 , T_j is the temp. of the dead state and is the temp. of the source corresponding to the heat transfer. Ignoring the kinetic and potential exergies, the following relation can be written as the sum of physical exergy (PE) and chemical exergy (CE) [23]:

$$\dot{E}x = \dot{E}x_{ph} + \dot{E}x_{ch} \quad (4)$$

The PE that depends on the pressure and temperature of a state is defined as below [23]:

$$\dot{E}x_{ph} = \dot{m}[(h - h_0) - T_0(s - s_0)] \quad (5)$$

In these equations, 0 in subscript refers to the dead state (DE), and s is the specific entropy of states. The CE of a stream is defined as the maximum work of it, when changes from a restricted DE to the real DE. The CE for an ig mixture is calculated as [23]:

$$\dot{E}x_{ch,mix} = \frac{\dot{m}}{MW_{mix}}(\sum_k y_k \bar{e}_k^{ch} + \bar{R}T_0 \sum_k y_k Ln y_k) \quad (6)$$

Where $\bar{e}_k^{ch}$ is the standard molar chemical exergy of component. Table 1 presents EBEs and EDR for each component of the single

SOFC-GT plant, and Table 2 presents EBEs and EDR for each component of the dual SOFC-GT plant.

B. SOFC electrochemical modeling

In a SOFC stack with internal reforming of methane, the following reactions take place [25]:

$$CH_4 + H_2O \leftrightarrow 3H_2 + CO \ (reforming) \quad (7)$$

$$CO + H_2O \leftrightarrow H_2 + CO_2 \ (shifting) \quad (8)$$

$$^1/_2O_2 + H_2 \leftrightarrow H_2O \ (Overallelectrochemicalreaction) \quad (9)$$

The reforming reaction (RR), unlike water-gas shifting (WGS) and electrochemical reactions, is endothermic. For this reason, the temperature distribution in the fuel cell is balanced. Because the reforming reaction consumes some of the heat produced by the other two reactions. This is an advantage for an internal reforming fuel cell because it will create less cooling load and fewer costs. The necessary steam for the reactions is provided by a recycled stream from the anode outlet into the cell. The important point here is to maintain the steam to carbon ratio (r_{sc}) of the cell, because if this parameter has a very small value, it will cause carbon deposition as well as deactivation of the catalyst. Steam to carbon ratio for the single SOFC-GT system is calculated as equation 10, and this ratio for the dual SOFC-GT system is defined as equations 11 and 12 [20]:

$$r_{sc} = \frac{\dot{n}_{H_2O,9}}{\dot{n}_{CH_4,7}+\dot{n}_{CO,9}} \quad (10)$$

$$r_{sc_1} = \frac{\dot{n}_{H_2O,11}}{\dot{n}_{CH_4,9}+\dot{n}_{CO,11}} \quad (11)$$

$$r_{sc_2} = \frac{\dot{n}_{H_2O,16}}{\dot{n}_{CH_4,14}+\dot{n}_{CO,16}} \quad (12)$$

The equilibrium constants of RR and WGS are defined as follows [26]:

$$K_{reform} = \frac{y_{CO}y_{H_2}^3}{y_{CH_4}y_{H_2O}}\left(\frac{P}{P_0}\right)^2 = \exp\left(-\frac{\Delta\bar{g}^0_{reform}}{\bar{R}T_{SOFC}}\right) \quad (13)$$

$$K_{shifting} = \frac{y_{CO_2}y_{H_2}}{y_{CO}y_{H_2O}} = \exp\left(-\frac{\Delta\bar{g}^0_{shifting}}{\bar{R}T_{SOFC}}\right) \quad (14)$$

Where $\bar{g}^0$ represents molar Gibbs free energy. Fuel utilization factor controls hydrogen consumption rate in the SOFC, and is calculated as [20]:

$$u_f = \frac{\gamma_r}{3\alpha_r+\beta_r+\dot{n}_{H_2,5}} \quad (15)$$

Where α_r, β_r and γ_r are conversion rate for Eqs. (7)-(10), respectively and γ_r can be obtained by Faraday's law [27]:

$$\gamma_r = \frac{j_{SOFC}N_{cell}A_{act}}{2F} \quad (16)$$

Wherej_{SOFC},N_{cell} and A_{act} are current density of cell, number of cells and cell active area, also implies Faraday constant. Other formulas for calculating voltage (V) are listed in Table 3. In the equations of this tableD_{eff},j_0 ,j_s,L, R,R_c, and ρ ate effective gas diffusion factor, exchange current density, limiting current density, thickness, universal gas constant, contact resistance, and electrical resistivity. In addition, the subscripts a, c, el, and int refer to anode, cathode, electrode, and interconnection.

C. Overall system analysis

The net power generation rate (PGR) of the plant is defined as below:

$$\dot{W}_{net} = \dot{W}_{SOFC} + \dot{W}_{GT} - \dot{W}_{AC} - \dot{W}_{FC} \quad (17)$$

Where $\dot{W}_{SOFC}$ is determined as [31]:

$$\dot{W}_{SOFC} = j_{SOFC}N_{cell}A_{act}V_{cell,SOFC} \quad (18)$$

The energy efficiency equation of the overall plant is [20]:

$\eta = \frac{\dot{W}_{net}}{\dot{n}_f.LHV}$ (19) Where $\dot{n}_f$ is molar rate of fuel and is the lower heating value of fuel. EDR of whole system is the sum of the EDR of each equipment and EDR of EG [23]:

$$\dot{E}x_{D,tot} = \sum_k \dot{E}x_{D,k} + \dot{E}x_{exhaust} \quad (20)$$

Exergy destruction ratio is defined as the portion of a component in the whole exergy destruction of system [23]:

$$Y_{D,k} = \frac{\dot{E}x_{D,k}}{\dot{E}x_{D,tot}} \quad (21)$$

Exergetic performance coefficient is the ratio of net PGR of the system to EDR of whole system [20]:

$$EPC = \frac{\dot{W}_{net}}{\dot{E}x_{D,tot}} \quad (22)$$

The unit emission of carbon dioxide, which is produced mainly in the burner, is defined as follows [32]:

$$EMI_{CO_2} = \frac{\dot{m}_{CO_2,emitted}}{\dot{W}_{net}} \times 3600 \quad (23)$$

4. RESULTS AND DISCUSSIONS

The results of the study are discussed in detail in this section. The single SOFC-GT plant is compared to the dual SOFC-GT plant from the energy, exergy, and environmental viewpoints. The effect of the FUF and fuel cell CD on the system performance and net power production were investigated. The analysis for of the system is conducted using EES software. Major system input data are summarized in Table 4. The exergy analysis shows that, for the operating condition considered, the afterburner with 49.1 kW for dual cell cycle and 30.52 kW in single cycle, have the maximum EDR in both systems. This was foresighted because of the significant irreversibilities associated with the chemical reactions. Fig.3 illustrates the share of each equipment in total EDR for the single SOFC-GT system, and Fig.4 shows this diagram for the dual SOFC-GT cycle. As can be seen, the mixers own a negligible share on the system exergy destruction because there is no reaction in them. In addition, the exergy destruction rate in both cycles indicates that the exhaust gas has a high rate of exergy destruction. This value is 62.02kW for a single cell cycle and 104.4kW for a dual cell cycle. Thus, the EDR of the whole plant in the single cell cycle and the dual cell cycle according to Equation 20 is 211.4kW and 384.1kW, respectively.

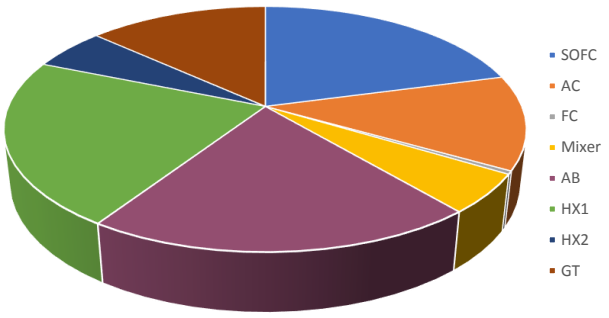

Fig. 3. portion of each equipment in exergy destruction for single SOFC-GT cycle

Table 1. EBEs and EDR for each equipment of single SOFC-GT plant

component	EBE	EDR
AC	$\dot{m}_2h_2 - \dot{m}_1h_1 = \dot{W}_{AC}$	$\dot{E}x_{D,AC} = \dot{m}_1ex_1 - \dot{m}_2ex_2 + \dot{W}_{AC}$
FC	$\dot{m}_6h_6 - \dot{m}_5h_5 = \dot{W}_{FC}$	$\dot{E}x_{D,FC} = \dot{m}_5ex_5 - \dot{m}_6ex_6 + \dot{W}_{FC}$
HX1	$\dot{m}_3h_3 + \dot{m}_{12}h_{12} = \dot{m}_4h_4 + \dot{m}_{13}h_{13}$	$\dot{E}x_{D.HX1} = \dot{m}_3ex_3 + \dot{m}_{12}ex_{12} - \dot{m}_4ex_4 - \dot{m}_{13}ex_{13}$
HX2	$\dot{m}_2h_2 + \dot{m}_{14}h_{14} = \dot{m}_3h_3 + \dot{m}_{15}h_{15}$	$\dot{E}x_{D.HX2} = \dot{m}_2ex_2 + \dot{m}_{14}ex_{14} - \dot{m}_3ex_3 - \dot{m}_{15}ex_{15}$
GT	$\dot{m}_{13}h_{13} - \dot{m}_{14}h_{14} = \dot{W}_{GT}$	$\dot{E}x_{D,GT} = \dot{m}_{13}ex_{13} - \dot{m}_{14}ex_{14} - \dot{W}_{GT}$
Mix	$\dot{m}_6h_6 + \dot{m}_9h_9 = \dot{m}_7h_7$	$\dot{E}x_{D,Mix} = \dot{m}_6ex_6 + \dot{m}_9ex_9 - \dot{m}_7ex_7$
AB	$\dot{m}_{10}h_{10} + \dot{m}_{11}h_{11} + \dot{W}_{AB} = \dot{m}_{12}h_{12}$	$\dot{E}x_{D,AB} = \dot{m}_{10}ex_{10} + \dot{m}_{11}ex_{11} - \dot{m}_{12}ex_{12}$
SOFC	$\dot{m}_7h_7 + \dot{m}_4h_4 = \dot{W}_{SOFC} + \dot{m}_8h_8 + \dot{m}_{11}h_{11}$	$\dot{E}x_{D,SOFC} = \dot{m}_4ex_4 + \dot{m}_7ex_7 - \dot{m}_8ex_8 - \dot{m}_{11}ex_{11} - \dot{W}_{SOFC}$

Table 2. EBEs and EDR for each equipment of dual SOFC-GT plant

component	EBE	EDR
AC	$\dot{m}_2h_2 - \dot{m}_1h_1 = \dot{W}_{AC}$	$\dot{E}x_{D,AC} = \dot{m}_1ex_1 - \dot{m}_2ex_2 + \dot{W}_{AC}$
FC	$\dot{m}_6h_6 - \dot{m}_5h_5 = \dot{W}_{FC}$	$\dot{E}x_{D,FC} = \dot{m}_5ex_5 - \dot{m}_6ex_6 + \dot{W}_{FC}$
HX1	$\dot{m}_3h_3 + \dot{m}_{22}h_{22} = \dot{m}_4h_4 + \dot{m}_{23}h_{23}$	$\dot{E}x_{D.HX1} = \dot{m}_3ex_3 + \dot{m}_{22}ex_{22} - \dot{m}_4ex_4 - \dot{m}_{23}ex_{23}$
HX2	$\dot{m}_2h_2 + \dot{m}_{24}h_{24} = \dot{m}_3h_3 + \dot{m}_{25}h_{25}$	$\dot{E}x_{D.HX2} = \dot{m}_2ex_2 + \dot{m}_{24}ex_{24} - \dot{m}_3ex_3 - \dot{m}_{25}ex_{25}$
GT	$\dot{m}_{23}h_{23} - \dot{m}_{24}h_{24} = \dot{W}_{GT}$	$\dot{E}x_{D,GT} = \dot{m}_{23}ex_{23} - \dot{m}_{24}ex_{24} - \dot{W}_{GT}$
Mix1	$\dot{m}_8h_8 + \dot{m}_{12}h_{12} = \dot{m}_9h_9$	$\dot{E}x_{D,Mix1} = \dot{m}_8ex_8 + \dot{m}_{17}ex_{17} - \dot{m}_9ex_9$
Mix2	$\dot{m}_7h_7 + \dot{m}_{18}h_{18} = \dot{m}_{15}h_{15}$	$\dot{E}x_{D,Mix2} = \dot{m}_7ex_7 + \dot{m}_{18}ex_{18} - \dot{m}_{15}ex_{15}$
Mix3	$\dot{m}_{13}h_{13} + \dot{m}_{19}h_{19} = \dot{m}_{21}h_{21}$	$\dot{E}x_{D,Mix3} = \dot{m}_{13}ex_{13} + \dot{m}_{19}ex_{19} - \dot{m}_{21}ex_{21}$
AB	$\dot{m}_{20}h_{20} + \dot{m}_{21}h_{21} + \dot{W}_{AB} = \dot{m}_{22}h_{22}$	$\dot{E}x_{D,AB} = \dot{m}_{20}ex_{20} + \dot{m}_{21}ex_{21} - \dot{m}_{22}ex_{22}$
SOFC1	$\dot{m}_{10}h_{10} + \dot{m}_4h_4 = \dot{W}_{SOFC1} + \dot{m}_{11}h_{11} + \dot{m}_{14}h_{14}$	$\dot{E}x_{D,SOFC1} = \dot{m}_4ex_4 + \dot{m}_{10}ex_{10} - \dot{m}_{14}ex_{14} - \dot{m}_{11}ex_{11} - \dot{W}_{SOFC1}$
SOFC2	$\dot{m}_{16}h_{16} + \dot{m}_{14}h_{14} = \dot{W}_{SOFC2} + \dot{m}_{17}h_{17} + \dot{m}_{20}h_{20}$	$\dot{E}x_{D,SOFC2} = \dot{m}_{14}ex_{14} + \dot{m}_{16}ex_{16} - \dot{m}_{20}ex_{20} - \dot{m}_{17}ex_{17} - \dot{W}_{SOFC2}$

Table 3. Electrochemical equations of solid oxide fuel cell

	Voltage equations [28-30]
Output Voltage	$V_{cell,SOFC} = V_N - V_{ohm} - V_{con,a} - V_{con,c} - V_{act,a} - V_{act,c}$
Nernst Voltage	$V_N = -\frac{\Delta^0}{2F} + \frac{T_{SOFC}}{2F}\ln(\frac{P_{H2}\sqrt{P_{O2}}}{P_{H2O}})$
Ohmic overpotential	$V_{ohm} = (R_C + \sum_i \rho_i L_i)j_{SOFC}$ $\rho_{el} = \left(\frac{3.34\times10^4}{T_{SOFC}}\exp\left(-\frac{10300}{T_{SOFC}}\right)\right)^{-1}$, $L_{el} = 0.001\times10^{-4}m$ $\quad$ $\rho_a = \left(\frac{95\times10^6}{T_{SOFC}}\exp\left(-\frac{1150}{T_{SOFC}}\right)\right)^{-1}$, $L_a = 0.05\times10^{-4}m$ $\rho_c = \left(\frac{42\times10^6}{T_{SOFC}}\exp\left(-\frac{1200}{T_{SOFC}}\right)\right)^{-1}$, $L_c = 0.005\times10^{-4}m$ $\quad$ $\rho_{int} = \left(\frac{9.3\times10^6}{T_{SOFC}}\exp\left(-\frac{1100}{T_{SOFC}}\right)\right)^{-1}$, $L_{int} = 0.3\times10^{-4}m$, $R_C = 0$
Anode activation overpotentoial	$V_{act,a} = \frac{T_{SOFC}}{F}\left(\sinh^{-1}\left(\frac{j_{SOFC}}{2j_{0,a}}\right)\right)$, $j_{0,a} = 6500A/m^2$
Cathode activation overpotential	$V_{act,c} = \frac{T_{SOFC}}{F}\left(\sinh^{-1}\left(\frac{j_{SOFC}}{2j_{0,c}}\right)\right)$, $j_{0,c} = 2500A/m^2$
Anode conc. overpotential	$V_{con,a} = \frac{\overline{R}T_{SOFC}}{2F}\left(\ln\left(1+\frac{P_{H2}\times j_{SOFC}}{P_{H2O}\times j_{s,a}}\right) - \ln\left(1-\frac{j_{SOFC}}{j_{s,a}}\right)\right)$ $j_{s,a} = \frac{2FP_{H2}D_{eff,a}}{T_{SOFC}L_a}$, $D_{eff,a} = 0.2\times10^{-4}m^2/s$
Cathode conc. overpotential	$V_{con,c} = -\left(\frac{T_{SOFC}}{4F}.\ln\left(1-\frac{j_{SOFC}}{j_{0,c}}\right)\right)$ $j_{s,c} = \frac{4FP_{O2}D_{eff,c}}{\left(\frac{P-P_{O2}}{P}\right)T_{SOFC}L_c}$, $D_{eff,c} = 0.05\times10^{-4}m^2/s$

Table 4. Input data for system modeling

parameter	value
Current density	2000 A/m^2
FCL temperature	1000 °C
FUF of each stack	0.8
Air utilization factor	0.17
Compression ratio	2.5
Cell active area	0.0834 m^2
Number of cells	1798
r_{sc}	2
Isentropic efficiency of compressor	85 %
Isentropic efficiency of turbine	85 %
After burner efficiency	98 %
HXs efficiency	85 %
Pressure drop in FCL	2 %
Pressure drop in heat exchangers	2 %
Pressure drop in after burner	3 %
Lower heating value of methane	808000 J/mol

Table 5. Some of modeling results

parameter	Single cell	Dual cell
First fuel cell voltage	0.7339 V	0.736 V
Second fuel cell voltage	-	0.7256 V
Heat generated in the first FCL	175.6 kW	175.6 kW
Heat generated in the second FCL	-	177.7 kW
Molar flowrate of input fuel	0.6461 mol/s	1.283 mol/s
Molar flowrate of input air	25.89 mol/s	28.77 mol/s

Some other modeling results, such as the voltage of FCLs for single and dual SOFC-GT plants, are listed in Table 5.

A. Parametric study

The influence of changing the main operating parameters of the system, including the CD and FUF of fuel cells, on the net power rate and energy efficiency of the plant, has been investigated. The effect of the CD of the second FCL on the net power generation rate is depicted in Fig.5 for three values of the current density of the first FCL. As shown in this figure, at a constant CD of 220 for cell 1, when the CD of cell 2 increases from 2400 to 2800 , the net power rises 54%. The relationship between the net power generation rate and the current density of cell 1 is also a direct relation. FUF of second FCL influence on the net PGR is investigated in Fig.6. As this figure shows, the PGR first increases to its maximum, and then, decreases by further increasing the FUF. However, the impact of the FUF of first cell is a direct effect on the net PGR. Fig.7 demonstrates the impact of changes in the second fuel cell CD in three different values of the first fuel cell CD on energy efficiency. Referring to this figure, the effect of CD

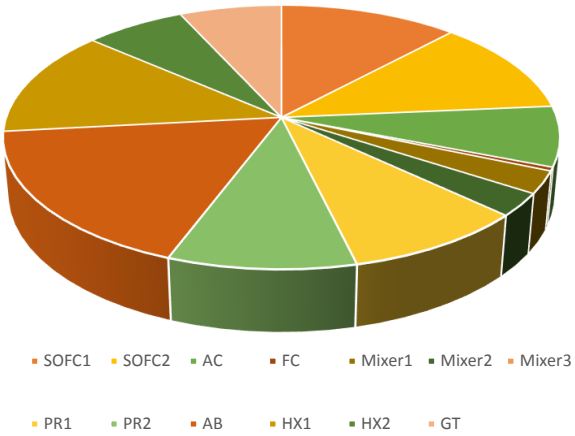

Fig. 4. portion of each equipment in exergy destruction for dual SOFC-GT cycle

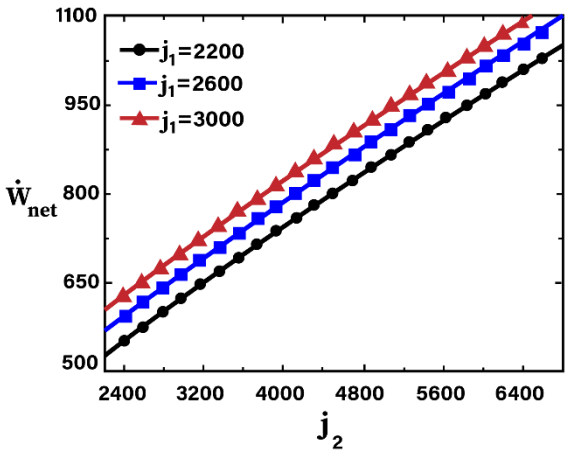

Fig. 5. Effect of CD on the net PGR

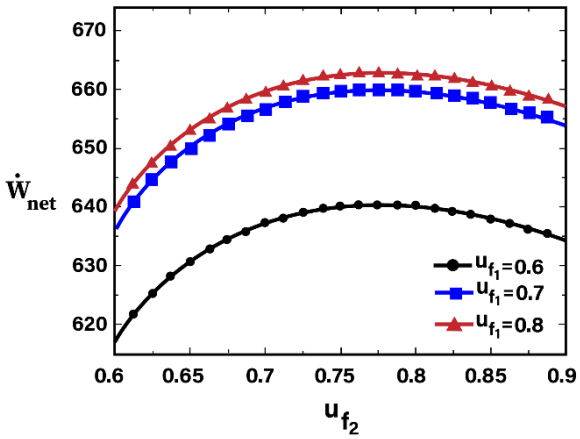

Fig. 6. Effect of FUF on the net PGR

of the second cell on system efficiency is not direct. when the CD of the first cell is assumed to be constant, the increase in current density of the second cell shows a maximum point in the graph;

however, as the CD of cell 1 increases, the efficiency of the system decreases when the CD of cell 2 is assumed to be constant. For example, for a constant CD of 2200 for the first cell, when the CD of the second cell increases from 2200 to 3100 , the efficiency of the system increases from 65% to 65.4%, but further increase in the CD, continuously reduces the efficiency and reaches 63.3% at a CD of 6400. Fig.8 shows the impact of changes in the FUF of

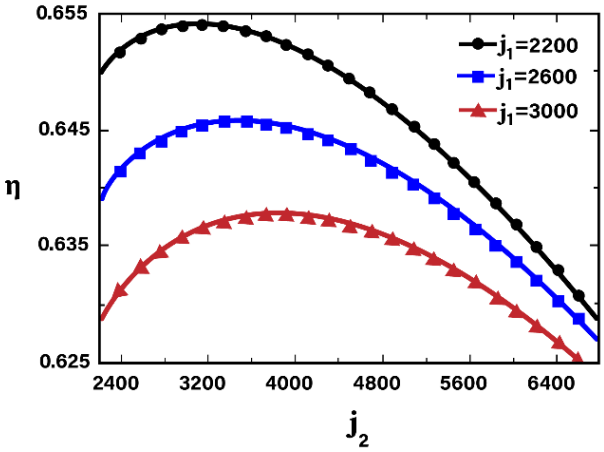

Fig. 7. Effect of CD on energy efficiency

the second fuel cell in three different values of the FUF of first fuel cell, on energy efficiency. As this diagram shows, energy efficiency increases as the FUF of the second cell increases, while the FUF of the first cell is constant. For example, increasing the FUF of cell 2 from 0.6 to 0.9, in a constant FUF of 0.6 for cell 1, increases the efficiency of the plant by approximately 14%. This relationship is also established for fuel cell 1, which means that energy efficiency increases with increasing FUF of the first cell, while the FUF of the second cell is constant. For example, increasing the FUF of cell 1 from 0.6 to 0.7, when this factor is kept constant and equal to 0.8 for the second cell, increases the efficiency from about 55% to about 61%.

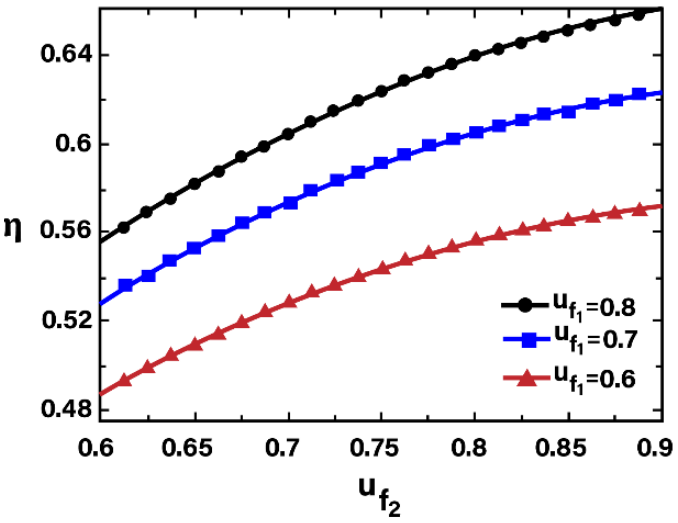

Fig. 8. Effect of FUF on energy efficiency

B. Comparative study

In this section, a comparative study between two single and dual SOFC-GT systems is performed. Fig.9 provides a comparison chart to compare the total EDR and net PGR rate for both systems. The net power generation rate for dual cell system is higher than for single cell system. This result is evident considering the design of these two systems. Because in the dual cell system, two cells are used, and also, the presence of pre reformers has a positive effect on the performance and power generation of the plant. Furthermore, the total exergy destruction rate for dual cell system is higher than for single cell system too. This is logical because of the significant irreversibilities associated with the chemical reactions that occur in three equipment; two fuel cells, and one afterburner The energy efficiency

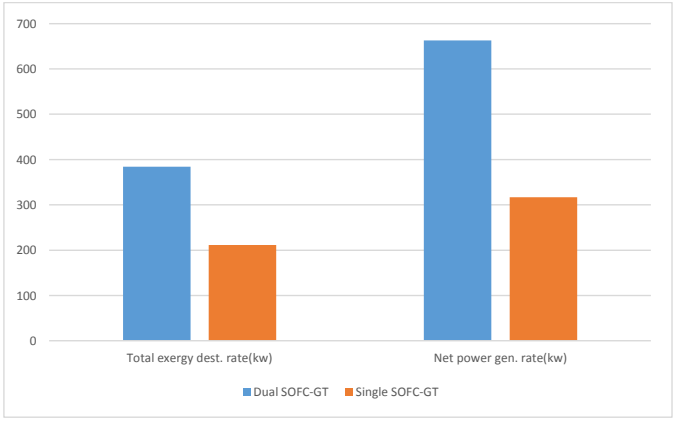

Fig. 9. Compare the total EDR and net PGR for both systems

and exergetic performance coefficient of both single and dual SOFC-GT systems are evaluated. Fig.10 shows that both of these parameters are affected in these systems. Referring to this figure, the energy efficiency and exergetic performance coefficient for dual cell system is higher than for single cell system. Fig. 11

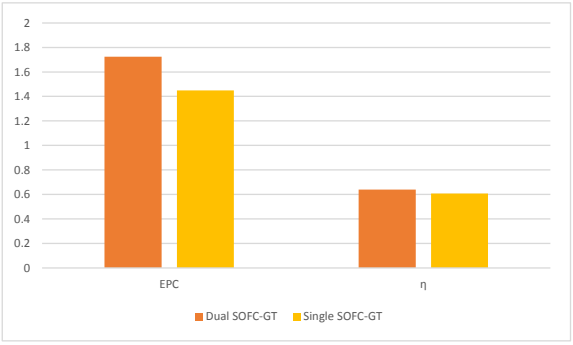

Fig. 10. Energy efficiency and exergetic performance coefficient comparison for systems

provides a comparison between power generation and power consumption rate in each cycle. As previously stated in Equation 17, the net PGR is equal to the generation rate of the cycle minus its consumption rate. Cycle power is generated by turbine and FCLs and consumed by compressors. As a result, the net power output rate for single cell cycle and dual cell cycle is 316.8kW and 662.6kW, respectively. Environmental analysis

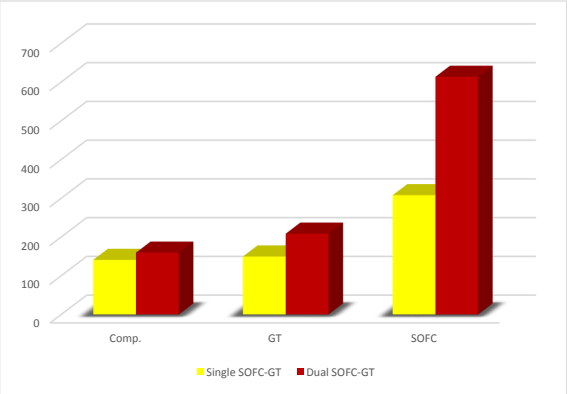

Fig. 11. Comparison between power generation and power consumption rate for systems

shows that the unit emission of carbon dioxide in single SOFC-GT system is equal to 323.165 $t.MW^{-1}h^{-1}$, while this value is 306.72 $t.MW^{-1}h^{-1}$ for dual SOFC-GT system. This result reveals that the dual cell cycle is safer for the environment than the single cell cycle.

5. CONCLUSIONS

A new dual SOFC-GT system is proposed and analyzed from a thermodynamic viewpoint in the present study. The result of energy analyses shows that the efficiency of this system is 63.93%, which is 3.24% higher than the single cell. Exergetic analyses demonstrate that the largest exergy destruction for both single and dual SOFC-GT cycle occur in afterburner, which is logical, because of the significant irreversibilities associated with the chemical reactions. Environmental analysis reveals that the Dual SOFC-GT system is more environmentally friendly than the single SOFC-GT system because it has a lower carbon dioxide emission rate. From the obtained theoretical results, the following conclusions are made:

- Although increasing the CD of second FCL leads to higher values of net power generation rate, further increasing deteriorates energy efficiency due to the increase of input fuel flowrate.
- There is a specific value of the current density of the second fuel cell on each constant current density of the first fuel cell in which energy efficiency is maximized.
- Increasing the FUF of the second fuel cell raises the efficiency of the system, but further increasing can decrease the net PGR of the plant.
- There is a distinct point of FUF of second FCL, on each constant FUF of first FCL, in which net PGR is maximized.
- Afterburner has the largest share of exergy destruction rate
- Calculations show a drop in power generation of about 5 kW at the generated power of the second FCL compared to the first cell in the dual cycle.

REFERENCES

1. P. Ahmadi and I. Dincer, "Thermodynamic and exergoenvironmental analyses, and multi-objective optimization of a gas turbine power plant," Applied Thermal Engineering, vol. 31, no. 14-15, pp. 2529-2540, 2011.
2. S. J. Zaidi and M. A. Rauf, "Fuel cell fundamentals," in Polymer membranes for fuel cells: Springer, 2009, pp. 1-6.
3. Y. Haseli, I. Dincer, and G. Naterer, "Thermodynamic modeling of a gas turbine cycle combined with a solid oxide fuel cell," International journal of hydrogen energy, vol. 33, no. 20, pp. 5811-5822, 2008.
4. M. Pan, K. Zhang, and X. Li, "Optimization of supercritical carbon dioxide based combined cycles for solid oxide fuel cell-gas turbine system: Energy, exergy, environmental and economic analyses," Energy Conversion and Management, vol. 248, p. 114774, 2021.
5. H. Ide, T. Yoshida, H. Ueda, and N. Horiuchi, "Natural gas reformed fuel cell power generation systems-a comparison of three system efficiencies," in Proceedings of the 24th intersociety energy conversion engineering conference, 1989: IEEE, pp. 1517-1522.
6. S. Harvey and H. Richter, "A detailed study of a gas turbine cycle with an integrated internal reforming solid oxide fuel cell," in Intersociety energy conversion engineering conference, 1994, p. 4231.
7. S. Chan, H. Ho, and Y. Tian, "Modelling of simple hybrid solid oxide fuel cell and gas turbine power plant," Journal of power sources, vol. 109, no. 1, pp. 111-120, 2002.
8. S. Chan, H. Ho, and Y. Tian, "Multi-level modeling of SOFC–gas turbine hybrid system," International Journal of Hydrogen Energy, vol. 28, no. 8, pp. 889-900, 2003.
9. F. Calise, A. Palombo, and L. Vanoli, "Design and partial load exergy analysis of hybrid SOFC–GT power plant," Journal of power sources, vol. 158, no. 1, pp. 225-244, 2006.
10. T. Araki, T. Ohba, S. Takezawa, K. Onda, and Y. Sakaki, "Cycle analysis of planar SOFC power generation with serial connection of low and high temperature SOFCs," Journal of Power Sources, vol. 158, no. 1, pp. 52-59, 2006.
11. M. Granovskii, I. Dincer, and M. A. Rosen, "Performance comparison of two combined SOFC–gas turbine systems," Journal of Power Sources, vol. 165, no. 1, pp. 307-314, 2007.
12. F. Calise, M. D. d'Accadia, A. Palombo, and L. Vanoli, "Simulation and exergy analysis of a hybrid solid oxide fuel cell (SOFC)–gas turbine system," Energy, vol. 31, no. 15, pp. 3278-3299, 2006.
13. P. Bórawski, A. Bełdycka-Bórawska, E. J. Szymańska, K. J. Jankowski, B. Dubis, and J. W. Dunn, "Development of renewable energy sources market and biofuels in The European Union," Journal of cleaner production, vol. 228, pp. 467-484, 2019.
14. C. Bang-Møller and M. Rokni, "Thermodynamic performance study of biomass gasification, solid oxide fuel cell and micro gas turbine hybrid systems," Energy Conversion and Management, vol. 51, no. 11, pp. 2330-2339, 2010.
15. S. Wongchanapai, H. Iwai, M. Saito, and H. Yoshida, "Performance evaluation of a direct-biogas solid oxide fuel cell-micro gas turbine (SOFC-MGT) hybrid combined heat and power (CHP) system," Journal of Power Sources, vol. 223, pp. 9-17, 2013.
16. S. F. Sghaier, T. Khir, and A. B. Brahim, "Energetic and exergetic parametric study of a SOFC-GT hybrid power plant," International Journal of Hydrogen Energy, vol. 43, no. 6, pp. 3542-3554, 2018.
17. N. Chitgar and M. Moghimi, "Design and evaluation of a novel multigeneration system based on SOFC-GT for electricity, fresh water and hydrogen production," Energy, vol. 197, p. 117162, 2020.
18. M. Beigzadeh, F. Pourfayaz, M. Ghazvini, and M. H. Ahmadi, "Energy and exergy analyses of solid oxide fuel cell-gas turbine hybrid systems fed by different renewable biofuels: A comparative study," Journal of Cleaner Production, vol. 280, p. 124383, 2021.
19. K. Atsonios et al., "Technical assessment of LNG based polygeneration systems for non-interconnected island cases using SOFC," International Journal of Hydrogen Energy, vol. 46, no. 6, pp. 4827-4843, 2021.
20. L. Khani, M. Mohammadpour, M. Mohammadpourfard, S. Z. Heris, and G. G. Akkurt, "Thermodynamic design, evaluation, and optimization of a novel quadruple generation system combined of a fuel cell, an absorption refrigeration cycle, and an electrolyzer," International Journal of Energy Research.
21. M. H. Taheri, L. Khani, M. Mohammadpourfard, and H. Aminfar, "Multi-objective optimization of a novel biomass-based multigeneration system consisting of liquid natural gas open cycle and proton exchange membrane electrolyzer," International Journal of Energy Research, 2021.

22. M. Udayakumar, "Studies of compressor pressure ratio effect on GAXAC (generator–absorber–exchange absorption compression) cooler," Applied Energy, vol. 85, no. 12, pp. 1163-1172, 2008.
23. A. Bejan, G. Tsatsaronis, and M. J. Moran, Thermal design and optimization. John Wiley & Sons, 1995.
24. F. Safari and I. Dincer, "Development and analysis of a novel biomass-based integrated system for multigeneration with hydrogen production," International Journal of Hydrogen Energy, vol. 44, no. 7, pp. 3511-3526, 2019.
25. A. Habibollahzade, Z. K. Mehrabadi, and E. Houshfar, "Exergoeconomic and environmental optimisations of multigeneration biomass-based solid oxide fuel cell systems with reduced CO2 emissions," International Journal of Energy Research, vol. 45, no. 7, pp. 10450-10477, 2021.
26. L. Khani, A. S. Mehr, M. Yari, and S. Mahmoudi, "Multi-objective optimization of an indirectly integrated solid oxide fuel cell-gas turbine cogeneration system," international journal of hydrogen energy, vol. 41, no. 46, pp. 21470-21488, 2016.
27. A. V. Akkaya, B. Sahin, and H. H. Erdem, "Exergetic performance coefficient analysis of a simple fuel cell system," International Journal of Hydrogen Energy, vol. 32, no. 17, pp. 4600-4609, 2007.
28. U. Bossel and L. Dubal, "Facts and figures, an International Energy Agency SOFC task report," 1992.
29. A. Habibollahzade, E. Gholamian, E. Houshfar, and A Behzadi, "Multi-objective optimization of biomass-based solid oxide fuel cell integrated with Stirling engine and electrolyzer," Energy conversion and management, vol. 171, pp. 1116-1133, 2018
30. J. W. Kim, A. V. Virkar, K. Z. Fung, K. Mehta, and S. C. Singhal, "Polarization effects in intermediate temperature, anode-supported solid oxide fuel cells," Journal of the Electrochemical Society, vol. 146, no. 1, p. 69, 1999.
31. M. Delpisheh, M. A. Haghghi, M. Mehrpooya, A. Chitsaz, and H. Athari, "Design and financial parametric assessment and optimization of a novel solar-driven freshwater and hydrogen cogeneration system with thermal energy storage," Sustainable Energy Technologies and Assessments, vol. 45, p. 101096, 2021.
32. E. Gholamian, P. Hanafizadeh, P. Ahmadi, and L. Mazzarella, "4E analysis and three-objective optimization for selection of the best prime mover in smart energy systems for residential applications: a comparison of four different scenarios," Journal of Thermal Analysis and Calorimetry, vol. 145, no. 3, pp. 887-907, 2021.